

OBCACHE: OPTIMAL BRAIN KV CACHE PRUNING FOR EFFICIENT LONG-CONTEXT LLM INFERENCE

Yuzhe Gu¹, Xiyu Liang³, Jiaojiao Zhao², Enmao Diao

¹University of Pennsylvania ²Duke University

³University of Electronic Science and Technology of China

tracygu@seas.upenn.edu, jz441@duke.edu

xiyuliang@std.uestc.edu.cn, diao_em@hotmail.com

ABSTRACT

Large language models (LLMs) with extended context windows enable powerful downstream applications but impose significant memory overhead, as caching all key-value (KV) states scales linearly with sequence length and batch size. Existing cache eviction methods address this by exploiting attention sparsity, yet they typically rank tokens heuristically using accumulated attention weights without considering their true impact on attention outputs. We propose Optimal Brain Cache (OBCACHE), a principled framework that formulates cache eviction as a layer-wise structured pruning problem. Building upon the Optimal Brain Damage (OBD) theory, OBCACHE quantifies token saliency by measuring the perturbation in attention outputs induced by pruning tokens, with closed-form scores derived for isolated keys, isolated values, and joint key-value pairs. Our scores account not only for attention weights but also for information from value states and attention outputs, thereby enhancing existing eviction strategies with output-aware signals. Experiments on LLaMA and Qwen models demonstrate that replacing the heuristic scores in existing works, which estimate token saliency across different query positions, with OBCACHE’s output-aware scores consistently improves long-context accuracy. Our code is available at this [link](#).

1 INTRODUCTION

Large language models (LLMs) (Touvron et al., 2023a;b; Bai et al., 2023a; OpenAI, 2023) have recently revolutionized a wide range of natural language processing tasks, including document summarization (Zhang et al., 2024a), question answering (Kamalloo et al., 2023), code generation (Roziere et al., 2023), and dialogue systems (Taori et al., 2023; Chiang et al., 2023). Despite their impressive capabilities, many of these applications require processing long sequences, which poses substantial challenges for efficient deployment. A major bottleneck in LLM inference stems from their autoregressive nature, which necessitates caching all key-value (KV) states across the context window. Because the cache size scales linearly with both sequence length and batch size, it leads to substantial memory and latency overheads. For instance, running a LLaMA-3.1-8B model (Grattafiori et al., 2024) with a 1M-token context window requires storing over 120GB of KV cache, which exceeds the memory capacity of most GPUs.

A promising line of research addresses this challenge via *KV cache eviction*, a training-free technique that reduces inference costs by selectively discarding unimportant KV tokens (Zhang et al., 2023; Xiao et al., 2024). These methods are motivated by the observation that only a small subset of tokens significantly influences model predictions. By evicting redundant tokens during inference, such approaches can substantially reduce memory and computation while incurring moderate performance degradation. Early methods such as H₂O (Zhang et al., 2023) evict tokens based on accumulated attention weights, a simple yet effective heuristic for estimating token saliency. More recent techniques, including TOVA (Oren et al., 2024) and SnapKV (Li et al., 2024), refine this strategy by introducing more sophisticated attention-based scoring mechanisms to better preserve accuracy. However, these methods rely primarily on attention weights and often overlook the role of value states in shaping the final model outputs. Heuristically accumulating attention scores fails to fully capture the true impact of token removal on attention outputs, which directly affects the hidden

states and downstream predictions. Consequently, such methods may mistakenly retain tokens with negligible influence or discard ones whose importance is not evident from attention weights alone.

To tackle these limitations, we propose Optimal Brain Cache (OBCACHE), a principled framework that formulates KV cache eviction as a layer-wise structured pruning problem. The key insight behind OBCACHE is that the actual impact of removing KV pairs, i.e., their influence on future model outputs, can be effectively approximated by analyzing local perturbations in historical attention outputs when the corresponding KV vectors are pruned. This approximation enables us to estimate the contribution of each token to the model output without requiring access to future states at inference time. Our analysis is grounded in the Optimal Brain Damage (OBD) theory (LeCun et al., 1989), originally proposed for pruning model weights. By treating cached keys and values as pruning variables, we define three types of pruning units: isolated value vectors, isolated key vectors, and joint key-value pairs at the same token position. In each case, we derive closed-form expressions for the pruning-induced output perturbation using a second-order Taylor approximation. These perturbation estimates serve as token-wise saliency scores to inform cache eviction and retention decisions.

In contrast to prior approaches, OBCACHE scores incorporate not only attention weights but also value states, pre-softmax attention logits, and attention outputs. This results in output-aware saliency measures that provide richer and more accurate signals for cache eviction. Furthermore, we show that existing attention-based scoring methods emerge as special cases under our framework. Specifically, the pruning objective is simplified to preserving the attention matrix, and the pruning units are reduced to individual attention columns. As such, OBCACHE generalizes and complements existing cache eviction methods, and can be seamlessly integrated into any score-based cache eviction pipeline to improve token selection.

We empirically demonstrate the effectiveness of OBCACHE through extensive experiments on long-context benchmarks. Specifically, we incorporate the three OBCACHE saliency scores into existing cache eviction frameworks, including H₂O, TOVA, and SnapKV. Across both LLaMA-3.1 and Qwen-2.5 models, we observe consistent performance improvements on a variety of long-context tasks, including Needle-in-a-Haystack passkey retrieval, long-sequence perplexity evaluation, and 16 benchmarks from LongBench (Bai et al., 2023b). Our results show that integrating OBCACHE scores can produce more accurate estimations of token saliency, significantly enhancing long-context inference performance while maintaining low computational overhead.

In summary, our key contributions are as follows:

- We introduce OBCACHE, a principled scoring framework for KV cache eviction that directly targets eviction-induced perturbations in attention outputs. The framework provides output-aware saliency measures that can be seamlessly integrated into existing cache eviction pipelines to improve token selection and saliency estimation.
- We provide the first theoretical formulation of KV cache eviction as a structured pruning problem, grounded in the classical Optimal Brain Damage (OBD) framework. Using a second-order Taylor approximation, we derive closed-form perturbation estimates for isolated keys, isolated values, and joint key-value pairs. This theoretical analysis also clarifies the limitations of prior attention-weight heuristics and shows that they can be interpreted as special cases of our more general formulation.
- We conduct extensive empirical studies demonstrating that replacing the heuristic scores in existing methods (H₂O, TOVA, SnapKV), which estimate token saliency across different query positions, with OBCACHE’s output-aware scores consistently improves performance on both LLaMA and Qwen models across diverse long-context benchmarks, including retrieval, perplexity evaluation, and LongBench tasks.

2 RELATED WORKS

KV Cache Compression. In long-context scenarios, reducing the size of the key-value (KV) cache is critical for optimizing the deployment of large language models (LLMs). To this end, *cache eviction* methods are motivated by the observation that only a sparse subset of tokens can significantly contribute to model predictions. For example, StreamingLLM (Xiao et al., 2024) identifies the *attention sink* phenomenon and retains both the initial and most recent tokens to enable infinite-context decoding. H₂O (Zhang et al., 2023) proposes accumulating attention weights across

all query positions to dynamically identify salient tokens. TOVA (Oren et al., 2024) simplifies this by considering only the attention distribution of the most recent query. A more refined strategy, SnapKV (Li et al., 2024), aggregates attention scores within a small observation window and applies a pooling-based clustering mechanism, which improves performance in retrieval-centric tasks. Orthogonal to eviction-based methods, Quest (Tang et al., 2024) retains the full KV cache and restricts attention computation to the most relevant tokens. CaM (Zhang et al., 2024b) and D₂O (Wan et al., 2025) aim to mitigate the information loss caused by irreversible eviction and merge evicted KV states into the retained cache. However, none of these approaches explicitly models the contribution of value states in estimating token importance, nor do they quantify the direct impact of KV removal on model outputs. In contrast, our method evaluates token saliency through output-aware perturbation analysis, providing a more principled and generalizable framework for cache eviction.

Model Pruning. Another direction for reducing LLM inference costs focuses on pruning model parameters. Classical pruning frameworks (LeCun et al., 1989; Hassibi & Stork, 1992) quantify the saliency of each pruning unit by estimating the perturbation it induces in a task-specific loss, often approximated to second order using a Taylor series. However, computing second-order statistics globally is still inefficient in LLM-scale models (Ma et al., 2023). To reduce complexity, recent approaches adopt local formulations that operate at the level of individual layers (Frantar & Alistarh, 2023; Sun et al., 2024), where the objective becomes minimizing the change in layer output. By varying the pruning units, such methods can structurally remove redundant components such as attention layers, heads, or hidden channels. In this work, we extend the layer-wise pruning paradigm to handle the eviction of the dynamic KV cache. By treating KV states as pruning units, we introduce a theoretically grounded framework to more accurately quantify token saliency.

3 OBCACHE

In this section, we present the details of OBCACHE. We begin by reviewing the workflow of key-value (KV) caching and formalizing the notation in Section 3.1. In Section 3.2, we introduce our formulation of cache eviction as a layer-wise structured pruning problem, with the objective of minimizing perturbations in attention outputs. Section 3.3 then presents our analytical solution to this perturbation minimization problem based on a second-order Taylor approximation. In Section 3.4, we show that our framework recovers existing attention-based scoring methods as special cases. Finally, we provide a qualitative example to highlight the effectiveness of our formulation in Section 3.5. An overview of the OBCACHE scoring mechanism is shown in Figure 1.

3.1 PRELIMINARIES ON LLM INFERENCE

We review the KV caching mechanism in transformer-based LLM inference, focusing on the prefill, decoding, and cache eviction phases. Bold capital letters denote matrices, and bold lowercase letters with subscripts denote row vectors. For clarity, we omit the batch, head, and layer indices.

Prefill Phase. Let $\mathbf{X} \in \mathbb{R}^{l \times d}$ denote the prompt embeddings, and let $\mathbf{Q}, \mathbf{K}, \mathbf{V} \in \mathbb{R}^{l \times d}$ be the corresponding projected query, key, and value matrices, where l is the prompt length and d is the hidden size. The attention output $\mathbf{O} \in \mathbb{R}^{l \times d}$ is computed as

$$\mathbf{O} = \mathbf{A}\mathbf{V}, \quad \mathbf{A} = \text{softmax}(\mathbf{Z}), \quad \mathbf{Z} = \frac{\mathbf{Q}\mathbf{K}^\top}{\sqrt{d}} \in \mathbb{R}^{l \times l},$$

where \mathbf{Z} denotes the pre-softmax attention logits and $\mathbf{A} \in \mathbb{R}^{l \times l}$ is the attention weight matrix. During this phase, the key and value matrices \mathbf{K} and \mathbf{V} are cached to avoid recomputation in subsequent decoding steps.

Decoding Phase. At decoding step t , let $\mathbf{x}_t \in \mathbb{R}^d$ be the newly generated token embedding, and let $\mathbf{q}_t, \mathbf{k}_t, \mathbf{v}_t \in \mathbb{R}^d$ be its projected query, key, and value vectors. After appending $\mathbf{k}_t, \mathbf{v}_t$ to the cache, the key and value matrices extend to shape $s \times d$, where $s = l + t$. The step- t attention output is

$$\mathbf{o}_s = \mathbf{a}_s \mathbf{V}, \quad \mathbf{a}_s = \text{softmax}(\mathbf{z}_s), \quad \mathbf{z}_s = \frac{\mathbf{q}_t \mathbf{K}^\top}{\sqrt{d}} \in \mathbb{R}^s.$$

For the remainder of this paper, we use $\mathbf{Q}, \mathbf{K}, \mathbf{V}, \mathbf{A}, \mathbf{O}$ to denote the full matrices corresponding to sequence length s , which reduces to prompt length l during the prefill phase when $t = 0$.

Cache Eviction. Eviction is triggered when the sequence length s of the KV cache exceeds a predefined budget N . After each forward pass, an eviction algorithm selects $s - N$ rows from \mathbf{K} and \mathbf{V} for permanent deletion. By enforcing a fixed cache budget, the model can decode arbitrarily long sequences while maintaining a bounded memory footprint.

3.2 CACHE EVICTION VIA PERTURBATION MINIMIZATION

Cache eviction can be viewed as a form of layer-wise structured pruning, where the saliency of each pruning unit (i.e., a key or a value vector) is quantified by the error it induces in the layer output. However, cache eviction introduces a unique challenge not encountered in classical model pruning: due to the autoregressive nature of generation, the actual error caused by removing a key–value pair at step s affects only future attention outputs, $\mathbf{o}_{s+1}, \mathbf{o}_{s+2}, \dots$, which are inaccessible at eviction time. We refer to this unobservable quantity as the *true eviction error*.

Although the true eviction error is not directly available, we observe that it can be effectively approximated by measuring perturbations in recent historical attention outputs, specifically $\mathbf{o}_s, \mathbf{o}_{s-1}, \dots$, when the corresponding KV vectors are pruned. We refer to this measurable surrogate as the *pruning-induced eviction error*, and use it as a proxy objective to estimate token saliency.

Building on this insight, we formulate cache eviction as a layer-wise structured pruning problem by treating \mathbf{V} and \mathbf{K} as pruning variables. Let $\hat{\mathbf{V}} = \mathbf{V} + \delta\mathbf{V}$ and $\hat{\mathbf{K}} = \mathbf{K} + \delta\mathbf{K}$ denote the perturbed value and key matrices after pruning, with resulting perturbed attention weights $\hat{\mathbf{A}}$ and outputs $\hat{\mathbf{O}}$. Our objective is to identify the token position p whose removal results in the minimal proxy loss:

$$\arg \min_p f(\hat{\mathbf{O}} - \mathbf{O}) \quad \text{s.t.} \quad \mathbf{e}_p^\top \delta\mathbf{V} + \mathbf{v}_p = \mathbf{0}, \quad \mathbf{e}_p^\top \delta\mathbf{K} + \mathbf{k}_p = \mathbf{0}, \quad (1)$$

where \mathbf{e}_p is a unit vector selecting the p -th row of $\delta\mathbf{V}$ and $\delta\mathbf{K}$, and $f(\cdot)$ is a norm function. Following prior work on model pruning (Sun et al., 2024), we adopt the squared Frobenius norm $\|\cdot\|_F^2$ for its smoothness. Under this formulation, the pruning-induced eviction error becomes:

$$\mathcal{L}(\hat{\mathbf{V}}, \hat{\mathbf{K}}) := \|\text{softmax}(\frac{\mathbf{Q}\hat{\mathbf{K}}^\top}{\sqrt{d}})\hat{\mathbf{V}} - \text{softmax}(\frac{\mathbf{Q}\mathbf{K}^\top}{\sqrt{d}})\mathbf{V}\|_F^2. \quad (2)$$

To highlight the effectiveness of our formulation, we present an empirical example in Section 3.5.

3.3 CACHE PRUNING SCORES

Directly recomputing the proxy error \mathcal{L} for every position p requires repeated attention operations and is computationally infeasible. Inspired by Optimal Brain Damage (OBD) (LeCun et al., 1989), we approximate \mathcal{L} via a second-order Taylor expansion around the unperturbed point (\mathbf{V}, \mathbf{K}) :

$$\mathcal{L}(\hat{\mathbf{V}}, \hat{\mathbf{K}}) = \frac{1}{2}\delta\mathbf{V}^\top \mathbf{H}_{vv} \delta\mathbf{V} + \frac{1}{2}\delta\mathbf{K}^\top \mathbf{H}_{kk} \delta\mathbf{K} + \delta\mathbf{V}^\top \mathbf{H}_{vk} \delta\mathbf{K} + \mathcal{O}(\|(\delta\mathbf{V}, \delta\mathbf{K})\|^3), \quad (3)$$

where $\mathbf{H}_{vv}, \mathbf{H}_{kk}, \mathbf{H}_{vk}$ are the Hessians of \mathcal{L} with respect to $\hat{\mathbf{V}}, \hat{\mathbf{K}}$, and their cross term. The first-order terms vanish at the expansion point since $\hat{\mathbf{O}} - \mathbf{O} = \mathbf{0}$. Due to the row-wise pruning constraint in Equation 1, only the p -th row of $\delta\mathbf{V}$ and $\delta\mathbf{K}$ are nonzero. Consequently, the off-diagonal Hessian blocks do not contribute to \mathcal{L} , which mirrors the diagonal assumption adopted in OBD. Thus, the output perturbation caused by pruning \mathbf{v}_p and \mathbf{k}_p further simplifies to

$$\mathbf{S}_p := \frac{1}{2}\mathbf{v}_p^\top [\mathbf{H}_{vv}]_{pp} \mathbf{v}_p + \frac{1}{2}\mathbf{k}_p^\top [\mathbf{H}_{kk}]_{pp} \mathbf{k}_p + \mathbf{v}_p^\top [\mathbf{H}_{vk}]_{pp} \mathbf{k}_p. \quad (4)$$

Here, \mathbf{S}_p defines the token-wise saliency score for the cached KV pair at position p . By explicitly evaluating the Hessian sub-blocks $[\mathbf{H}_{vv}]_{pp}$, $[\mathbf{H}_{kk}]_{pp}$, and $[\mathbf{H}_{vk}]_{pp}$, we derive closed-form eviction scores that are both interpretable and efficient to compute.

The perturbation in Equation 4 captures the joint impact of pruning both \mathbf{v}_p and \mathbf{k}_p . We also consider simplified variants where either \mathbf{v}_p or \mathbf{k}_p is pruned independently while the other remains fixed. As a result, OBCACHE features three output-aware saliency scores:

Value-Pruning Score. When only the value vector \mathbf{v}_p is the pruning unit, the error reduces to the first term in Equation 4. Substituting the corresponding Hessian gives the value-pruning score:

$$\mathbf{S}_p^{\text{value}} = \sum_i |\mathbf{A}_{i,p}|^2 \cdot \|\mathbf{v}_p\|^2. \quad (5)$$

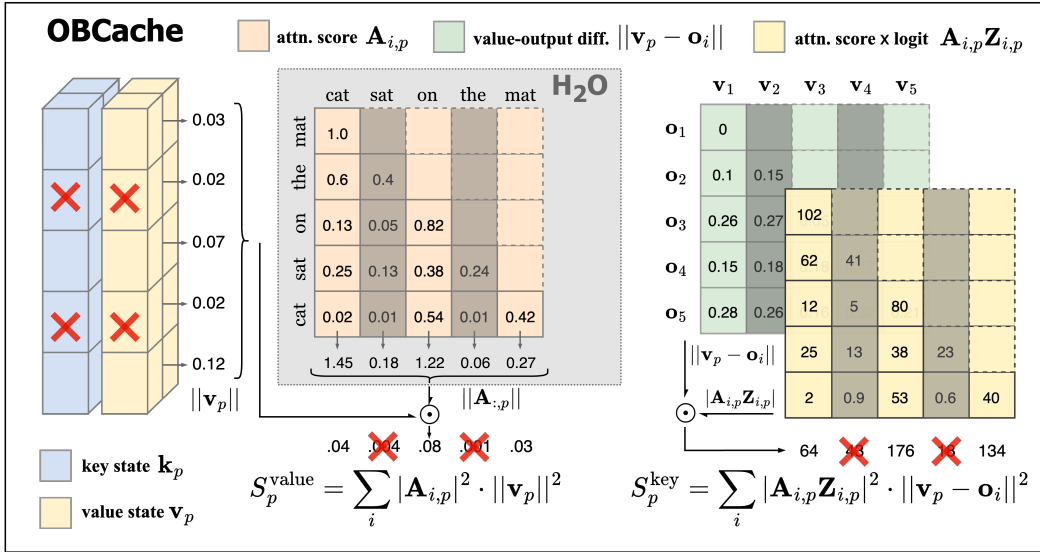


Figure 1: Overview of the OBCACHE scoring mechanism. The diagram shows the eviction process using value-pruning (left) and key-pruning scores (right). Unlike prior methods based solely on attention statistics (gray region), OBCACHE further incorporates value states, attention logits, and outputs to estimate token saliency, explicitly targeting the minimization of eviction-induced errors.

This score corresponds to the squared L_2 -norm of the p -th column of the attention weight matrix, scaled by the squared L_2 -norm of the value vector \mathbf{v}_p .

Key-Pruning Score. When only the key vector \mathbf{k}_p is considered as the pruning unit, the error reduces to the second term of Equation 4, resulting in the key-pruning score:

$$S_p^{\text{key}} = \sum_i |\mathbf{A}_{i,p} \cdot \mathbf{Z}_{i,p}|^2 \cdot \|\mathbf{v}_p - \mathbf{o}_i\|^2. \quad (6)$$

This score captures the deviation between the value vector and attention output, weighted by both the attention weights and the pre-softmax logits. Key pruning generally incurs larger errors than value pruning, as it alters the entire attention distribution.

Joint-Pruning Score. When \mathbf{v}_p and \mathbf{k}_p are treated as a combined pruning unit, the saliency score includes a cross-term in addition to the individual contributions:

$$S_p^{\text{joint}} = 2 \sum_i |\mathbf{A}_{i,p}|^2 \cdot \mathbf{Z}_{i,p} \cdot (\|\mathbf{v}_p\|^2 - \mathbf{v}_p^\top \mathbf{o}_i) + S_p^{\text{value}} + S_p^{\text{key}}. \quad (7)$$

This expression captures the combined and interactive effects of pruning the key and value vectors, providing the most comprehensive estimate of the pruning-induced eviction error.

These scores can be applied during both prefill and decoding phases. In particular, by accumulating scores over time, OBCACHE can support real-time updates to token-wise saliency, enabling dynamic KV cache eviction as decoding progresses. A complete derivation is provided in Appendix B.

3.4 CONNECTION TO EXISTING METHODS

Our framework naturally recovers existing attention-based eviction strategies as special cases. To show this, we introduce an additional index $w \in [1, s]$ and use $\mathbf{A}_{w:s}$ to denote the rows of the attention matrix \mathbf{A} corresponding to the query positions from w to s . Consider an alternative formulation that minimizes perturbations not in the attention outputs \mathbf{O} , but in the historical attention rows $\mathbf{A}_{w:s}$. In this case, minimizing the pruning-induced error reduces to:

$$\arg \min_p \|\hat{\mathbf{A}}_{w:s} - \mathbf{A}_{w:s}\|_{1,1} \quad \text{s.t.} \quad \delta \mathbf{A}_{w:s} \mathbf{e}_p + \mathbf{A}_{w:s,p} = \mathbf{0}, \quad (8)$$

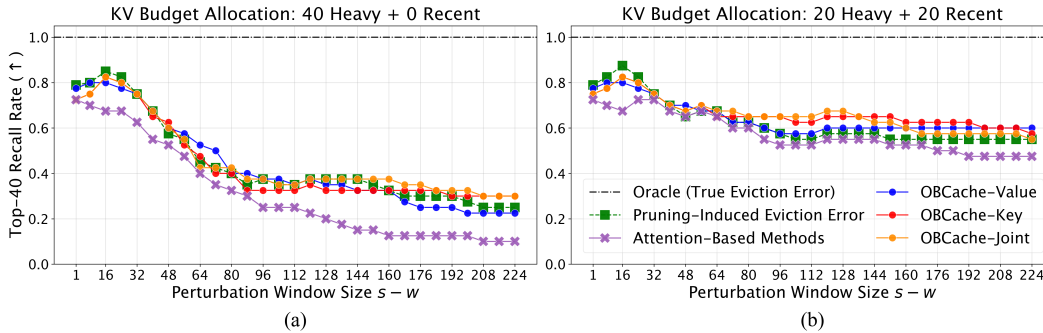


Figure 2: Recall rate of the top-40 salient tokens identified by the oracle eviction error. Results are collected from a 4K-context passkey retrieval task using LLaMA-3.2-3B-Instruct. The left plot (a) shows recall of top-40 tokens selected by different scoring methods. The right plot (b) demonstrates how allocating a fixed recent window improves oracle recall when perturbation windows are large, mitigating the structural bias disproportionately favoring earlier tokens.

where the pruning unit also simplifies to a column of the attention matrix. We refer to query positions from w to s as the *perturbation window*. Solving Equation 8 leads to a saliency score of the form:

$$\mathcal{S}_p^{\text{attn-based}} = \sum_{i=w}^s |\mathbf{A}_{i,p}|, \quad (9)$$

which corresponds to an L_1 -norm variant of our value-pruning score $\mathcal{S}_p^{\text{value}}$, but without incorporating any value-state information. This formulation connects directly to several recent methods. Specifically, H₂O (Zhang et al., 2023) sets $w = 1$, accumulating attention weights over the entire sequence history. TOVA (Oren et al., 2024) sets $w = s$, targeting only the most recent query position. SnapKV (Li et al., 2024) adopts a short window (i.e., $w \gg 1$), emphasizing recent attentions. By varying the choice of w , these methods effectively target different perturbation windows.

In OBCACHE, when we also relax the objective to the output error within the perturbation window:

$$\arg \min_p \|\widehat{\mathbf{O}}_{w:s} - \mathbf{O}_{w:s}\|_F^2 \quad \text{s.t.} \quad \mathbf{e}_p^\top \delta \mathbf{V} + \mathbf{v}_p = \mathbf{0}, \quad \mathbf{e}_p^\top \delta \mathbf{K} + \mathbf{k}_p = \mathbf{0}, \quad (10)$$

the resulting scores also become localized to the same set of query positions w through s . Therefore, OBCACHE generalizes these prior approaches by further introducing output-aware signals, enabling more informed eviction decisions that go beyond raw attention statistics.

3.5 EFFECTIVENESS OF PRUNING-INDUCED EVICTION ERROR

To further support our pruning-based formulation for cache eviction, we present a qualitative analysis on a passkey retrieval task, as shown in Figure 2. We begin by establishing an oracle baseline based on the *true eviction error*, which is measured as the perturbation in the first decoding-step output \mathbf{o}_{l+1} caused by evicting each cached token during the prefill phase. The top- k tokens with the largest oracle errors are treated as ground-truth important positions.

To evaluate the effectiveness of the *pruning-induced eviction error* as a proxy, we compute Equation 2 exactly for each candidate position in the prefill phase and select the top- k accordingly. As shown in the figure, when the perturbation window is appropriately chosen, the proxy achieves up to 85% recall of the oracle top- k selections. Next, we demonstrate the superiority of OBCACHE. Although derived via second-order Taylor approximation, OBCACHE scores achieve nearly identical ranking performance to the exact proxy, while being significantly more efficient due to their closed-form expression. Compared to attention-based methods, our scores consistently yield higher oracle recall, showcasing the benefit of incorporating output-aware signals into saliency estimation.

We observe that recall degrades when the perturbation window becomes larger. This issue stems from attention causality: earlier tokens attend to more queries and thus accumulate disproportionately higher saliency scores, introducing a structural bias that favors retaining initial tokens. To mitigate this, H₂O reserves a portion of the cache budget for a recent window, ensuring that the

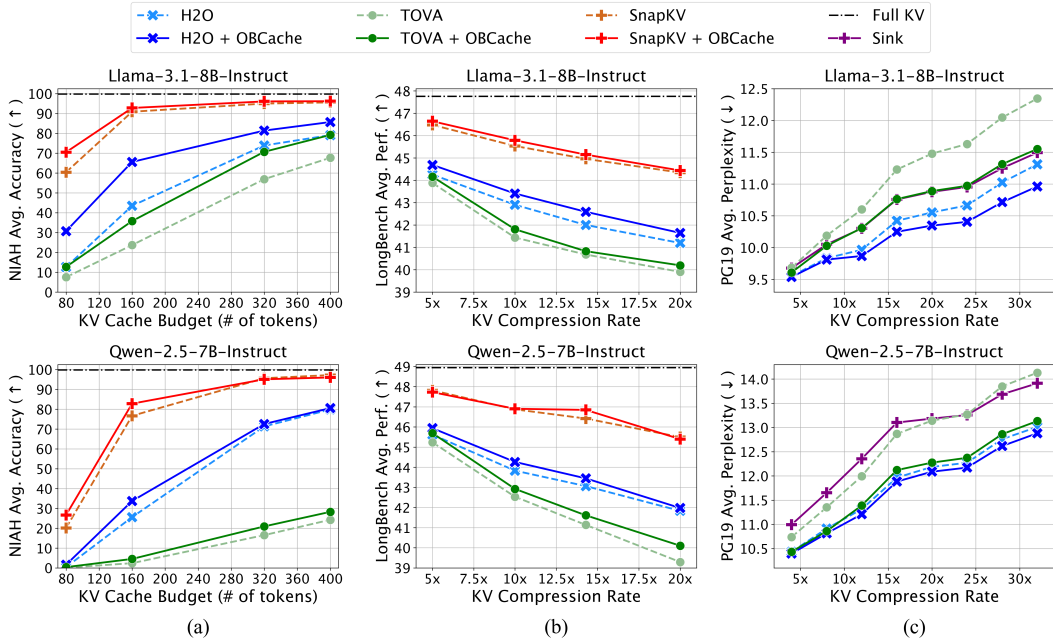


Figure 3: Overall long-context performance evaluation of LLaMA and Qwen. When integrated with OBCACHE scores, existing cache eviction baselines achieve superior compression and performance trade-off on the Needle-In-A-Haystack (a), LongBench (b), and perplexity (c) benchmarks.

most recent tokens are never evicted. This policy is also complementary to OBCACHE, and we find that recall further improves when a fixed 20-token window is reserved, as demonstrated in Figure 2b.

4 EXPERIMENTS

In this section, we conduct comprehensive experiments to evaluate the effectiveness of OBCACHE in enhancing existing score-based cache eviction methods, thereby improving performance across a range of long-context benchmarks. We evaluate OBCACHE for both static cache eviction in the prefill phase (Section 4.2) and dynamic cache eviction in the decoding phase (Section 4.3).

4.1 EXPERIMENTAL SETUP

Datasets. For prefill-phase cache eviction, we adopt two widely recognized long-context benchmarks: Needle-in-a-Haystack (NIAH) (Kamradt, 2023) and LongBench (Bai et al., 2023b). NIAH tests a model’s ability to retrieve a small but crucial “needle” randomly embedded in a lengthy document. Our implementation follows the RULER benchmark (Hsieh et al., 2024) and we evaluate across multiple context lengths (from 4K to 32K) under varying cache budgets. LongBench evaluates LLM’s long-context understanding via 16 datasets spanning six task categories: single-document QA, multi-document QA, summarization, few-shot learning, synthetic reasoning, and code completion. The average input length across all datasets is 6,711 words, making KV cache optimization critical during inference. For decoding-phase cache eviction, we follow the setup in StreamingLLM (Xiao et al., 2024), and report language modeling perplexity on PG19 (Rae et al., 2019), a dataset of 100 books with an average length of 70K tokens.

Baselines. We compare OBCACHE with three state-of-the-art cache eviction methods: H₂O (Zhang et al., 2023), TOVA (Oren et al., 2024), and SnapKV (Li et al., 2024), all of which rely solely on attention statistics but differ in eviction strategy. H₂O accumulates historical attention weights while retaining a fixed window of recent tokens. TOVA selects tokens based solely on the most recent query’s attention weights and does not require a recent window. SnapKV, designed for prefill-only eviction, scores tokens based on a recent attention window and applies pooling to smooth token importance, making it effective for retrieval-centric tasks. We integrate OBCACHE into these

Table 1: Results of the Needle-in-a-Haystack test on LLaMA-3.1-8B-Instruct. Each accuracy value corresponds to exact match over 250 random samples drawn from the RULER benchmark.

KV Budget (# tokens)	4K Context				8K Context				16K Context				32K Context				Avg.
	80	160	320	400	80	160	320	400	80	160	320	400	80	160	320	400	
H2O	7.6	36.8	68.0	77.2	10.8	47.2	75.2	79.2	14.8	45.2	80.0	82.8	17.2	44.8	72.4	77.2	52.28
+ OBCACHE-VALUE	15.2	54.4	76.8	82.4	21.6	60.4	82.4	85.2	30.8	72.0	84.4	85.6	32.4	61.6	82.4	86.4	63.38
+ OBCACHE-KEY	19.2	55.6	77.2	84.0	29.6	60.4	82.8	86.8	39.6	70.8	83.6	84.8	35.2	65.2	84.0	88.0	65.42
+ OBCACHE-JOINT	25.6	62.0	77.6	82.8	33.2	67.2	83.2	88.0	34.4	72.0	82.0	84.8	29.6	61.2	82.8	87.2	65.85
TOVA	7.2	24.4	63.6	76.0	9.2	26.4	62.4	68.8	6.8	21.6	55.6	68.0	6.8	22.4	46.0	58.0	38.95
+ OBCACHE-VALUE	12.4	34.4	75.6	84.0	10.4	37.6	71.6	81.2	10.0	34.4	67.6	77.2	14.4	31.6	61.2	68.4	48.25
+ OBCACHE-KEY	12.8	37.2	78.0	86.4	12.4	38.0	73.6	82.8	12.0	34.8	69.2	79.2	15.2	34.0	60.4	68.4	49.65
+ OBCACHE-JOINT	10.4	34.0	75.2	85.2	12.8	39.2	74.4	80.4	12.8	37.6	69.6	78.8	14.8	32.4	63.6	72.4	49.60
SnapKV	66.4	84.8	92.8	93.2	58.4	92.0	96.4	97.2	55.6	90.8	94.0	95.2	61.2	96.0	96.8	96.8	85.48
+ OBCACHE-VALUE	64.4	83.6	92.4	92.8	63.6	92.4	96.8	97.2	60.0	89.2	93.6	94.4	64.0	93.2	96.8	97.2	85.72
+ OBCACHE-KEY	73.6	82.8	92.4	92.4	72.8	92.4	97.2	96.4	70.8	93.6	96.0	96.0	74.0	96.8	96.8	97.2	88.82
+ OBCACHE-JOINT	68.4	86.4	92.0	92.8	72.0	95.2	97.6	96.8	73.6	95.6	96.8	97.2	68.0	94.0	98.0	98.0	88.90

baselines by replacing their attention-based scores with our perturbation-aware scores while preserving their original eviction strategies. We refer to our eviction methods using the value-pruning score (Equation 5) as OBCACHE-VALUE, the key-pruning score (Equation 6) as OBCACHE-KEY, and joint pruning score (Equation 7) as OBCACHE-JOINT, respectively.

Implementation Details. We use LLaMA-3.1-8B-Instruct (Grattafiori et al., 2024) and Qwen-2.5-7B-Instruct (Bai et al., 2023a) as our backbone LLMs, both of which natively supports 128K context windows. All experiments are implemented using the HuggingFace Transformers library (Wolf et al., 2020) with PyTorch (Paszke et al., 2019). To improve efficiency, we modify existing baseline’s prefill-phase attention operation using FlashAttention-2 (Dao, 2023), which reduces memory overhead for long-context samples. For prefill-phase eviction, we follow setups in SnapKV, where cache eviction occurs only once before decoding begins. This reflects real-world scenarios where prefill KV cache dominates memory usage compared to the ones in decoding. For decoding-phase eviction, we follow H₂O to fix a recent window, while evicting tokens at every step to evaluate the dynamic impact of different saliency scores. Full implementation details are provided in Appendix C.

4.2 PREFILL CACHE EVICTION

Needle-In-A-Haystack Results. Table 1 presents detailed NIAH passkey retrieval accuracy under different cache budgets and context lengths, comparing baseline eviction methods with their OBCACHE-enhanced counterparts. In addition, we aggregate accuracies over all context sizes and present the compression-performance trade-off curves for OBCACHE-JOINT in Figure 3a.

Across all baselines, compression rates, and context lengths, integrating OBCACHE scores consistently improves the retrieval accuracy. In particular, when applied to H₂O and TOVA, OBCACHE yields substantial accuracy gains, achieving over $1.26\times$ the original accuracy. These increments are more significant under extreme compression rates, highlighting the advantage of output-aware scores in identifying critical tokens. For SnapKV, the improvement is relatively smaller (3% absolute increase) as it already performs near saturation. However, under severe compression settings (e.g., 80-token budgets), OBCACHE still achieves 10% absolute gains as depicted in Figure 3a. These results demonstrate the robustness of OBCACHE scores in constrained memory settings. Overall, all three baselines benefit from the integration of OBCACHE at every tested compression rate, which highlights the advantage of our output-aware scoring mechanism over attention-based heuristics.

In addition to the comparison with baselines, Table 1 also provides an ablation on OBCACHE’s three score variants, derived via different pruning unit assumptions. We observe that eviction scores derived from key pruning, i.e., OBCACHE-KEY and OBCACHE-JOINT, tend to outperform the value-only variant OBCACHE-VALUE. This aligns with our expectation that pruning keys has greater impact, due to their role in shaping attention distributions and ultimately the model predictions. Accounting for key sensitivity thus yields more accurate saliency estimates and better performance. Although the OBCACHE-VALUE variant underperforms slightly, it remains appealing for its simplicity: it requires only an additional scaling factor based on value-state norms, making it nearly as efficient as baseline attention scores while still delivering substantial performance gains.

LongBench Results. We report the full table of results across all 16 LongBench datasets when retaining only 5%, 10%, 20% of the KV tokens in Appendix E.1. To highlight the benefits of OBCACHE, we also present the average task performance across different compression rates in Figure 3b. For both LLaMA-3.1 and Qwen-2.5 models, we observe consistent improvements in average performance when integrating OBCACHE into existing baselines. Interestingly, the improvement for SnapKV on Qwen is relatively smaller. We hypothesize that this is due to SnapKV’s pooling-based smoothing mechanism providing limited additional benefit when applied to our key-pruning scores, which already capture more nuanced token saliency beyond raw attention statistics. Overall, the results confirm that replacing attention-only scores with OBCACHE saliency enables more effective preservation of task-critical tokens under various compression levels.

4.3 DYNAMIC CACHE EVICTION

Beyond static prefill-phase cache eviction, OBCACHE is also applicable to decoding-time scenarios, where eviction decisions must be made dynamically. To evaluate this, we measure language modeling perplexity at varying sequence lengths on the PG19 dataset, using a fixed KV cache budget of 1024 tokens. Following Xiao et al. (2024), we allocate 4 fixed initial tokens for all methods, as these tokens act as attention sinks and are crucial for long-sequence generation quality. As demonstrated in Figure 4, the Sink baseline, which statically allocates the cache to fixed initial and recent tokens, demonstrates the highest perplexity. The H₂O baseline, which dynamically selects important tokens based on cumulative attention statistics, performs moderately better. In contrast, all OBCACHE variants, which also accumulate output-aware scores over time, consistently outperform H₂O across all sequence lengths. As observed, OBCACHE-JOINT does not yield better performance than OBCACHE-KEY, suggesting that a better combination of key and value pruning scores may exist beyond the current plain additive formulation. SnapKV is not evaluated as it does not support decoding-phase eviction. We also present the perplexity-compression trade-off curves in Figure 3c, where baselines integrated with OBCACHE scores all exhibit consistently lower perplexity at all compression levels. These results confirm that our perturbation-aware saliency scores can improve memory utilization and preserve long-range dependencies critical for continuous generation.

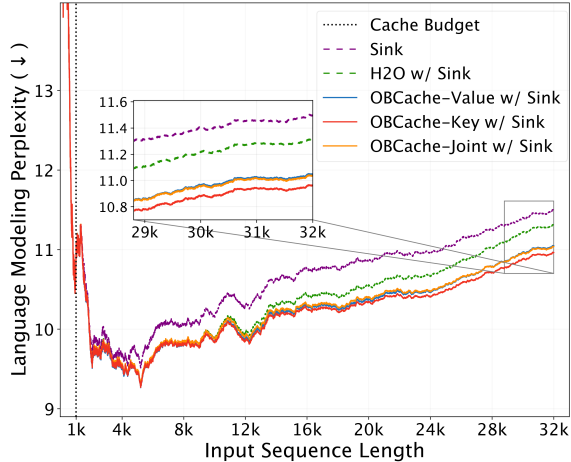


Figure 4: Language modeling perplexity evaluation on PG19 test set. We prompt Llama-3.1-8B-Instruct with 1 to 32K tokens and measure the perplexity of output tokens at varying context lengths. The KV cache budget for all methods is fixed at 1024 number of tokens.

5 CONCLUSION

In this work, we introduce OBCACHE, a principled framework for KV cache eviction in large language model inference, grounded in a perturbation minimization perspective. By casting cache eviction as a layer-wise structured pruning problem, we derived token saliency scores that aim to minimize the impact of removal on attention outputs. Extensive experiments across both prefilling and decoding scenarios on long-context benchmarks demonstrate that OBCACHE consistently outperforms state-of-the-art baselines, achieving superior performance-compression trade-offs, particularly under tight memory budgets. OBCACHE also offers a flexible foundation for principled KV cache compression: its structured pruning framework can be extended to other settings by modifying the pruning objective or unit. For instance, one could adapt OBCACHE to channel-wise KV pruning, or explore cache merging strategies by relaxing the diagonal approximation in our analysis. These directions open promising paths towards more effective and theoretically grounded KV cache management in long-context LLMs.

REFERENCES

- Jinze Bai, Shuai Bai, Yunfei Chu, Zeyu Cui, Kai Dang, Xiaodong Deng, Yang Fan, Wenbin Ge, Yu Han, Fei Huang, et al. Qwen technical report. *arXiv preprint arXiv:2309.16609*, 2023a.
- Yushi Bai, Xin Lv, Jiajie Zhang, Hongchang Lyu, Jiankai Tang, Zhidian Huang, Zhengxiao Du, Xiao Liu, Aohan Zeng, Lei Hou, et al. Longbench: A bilingual, multitask benchmark for long context understanding. *arXiv preprint arXiv:2308.14508*, 2023b.
- Wei-Lin Chiang, Zhuohan Li, Ziqing Lin, Ying Sheng, Zhanghao Wu, Hao Zhang, Lianmin Zheng, Siyuan Zhuang, Yonghao Zhuang, Joseph E Gonzalez, et al. Vicuna: An open-source chatbot impressing gpt-4 with 90%* chatgpt quality. See <https://vicuna.lmsys.org> (accessed 14 April 2023), 2(3):6, 2023.
- Tri Dao. Flashattention-2: Faster attention with better parallelism and work partitioning. *arXiv preprint arXiv:2307.08691*, 2023.
- Elias Frantar and Dan Alistarh. Sparsegpt: Massive language models can be accurately pruned in one-shot. In *International conference on machine learning*, pp. 10323–10337. PMLR, 2023.
- Aaron Grattafiori, Abhimanyu Dubey, Abhinav Jauhri, Abhinav Pandey, Abhishek Kadian, Ahmad Al-Dahle, Aiesha Letman, Akhil Mathur, Alan Schelten, Alex Vaughan, et al. The llama 3 herd of models. *arXiv preprint arXiv:2407.21783*, 2024.
- Babak Hassibi and David Stork. Second order derivatives for network pruning: Optimal brain surgeon. *Advances in neural information processing systems*, 5, 1992.
- Cheng-Ping Hsieh, Simeng Sun, Samuel Krirman, Shantanu Acharya, Dima Rekish, Fei Jia, Yang Zhang, and Boris Ginsburg. Ruler: What’s the real context size of your long-context language models? *arXiv preprint arXiv:2404.06654*, 2024.
- Ehsan Kamalloo, Nouha Dziri, Charles LA Clarke, and Davood Rafiei. Evaluating open-domain question answering in the era of large language models. *arXiv preprint arXiv:2305.06984*, 2023.
- Greg Kamradt. Needle in a haystack-pressure testing llms. *GitHub repository*, pp. 28, 2023.
- Yann LeCun, John Denker, and Sara Solla. Optimal brain damage. *Advances in neural information processing systems*, 2, 1989.
- Yuhong Li, Yingbing Huang, Bowen Yang, Bharat Venkitesh, Acyr Locatelli, Hanchen Ye, Tianle Cai, Patrick Lewis, and Deming Chen. Snapkv: Llm knows what you are looking for before generation. *Advances in Neural Information Processing Systems*, 37:22947–22970, 2024.
- Xinyin Ma, Gongfan Fang, and Xinchao Wang. Llm-pruner: On the structural pruning of large language models. *Advances in neural information processing systems*, 36:21702–21720, 2023.
- R OpenAI. Gpt-4 technical report. arxiv 2303.08774. *View in Article*, 2(5):1, 2023.
- Matanel Oren, Michael Hassid, Nir Yarden, Yossi Adi, and Roy Schwartz. Transformers are multi-state rnns. *arXiv preprint arXiv:2401.06104*, 2024.
- Adam Paszke, Sam Gross, Francisco Massa, Adam Lerer, James Bradbury, Gregory Chanan, Trevor Killeen, Zeming Lin, Natalia Gimelshein, Luca Antiga, et al. Pytorch: An imperative style, high-performance deep learning library. *Advances in neural information processing systems*, 32, 2019.
- Jack W Rae, Anna Potapenko, Siddhant M Jayakumar, and Timothy P Lillicrap. Compressive transformers for long-range sequence modelling. *arXiv preprint arXiv:1911.05507*, 2019.
- Baptiste Roziere, Jonas Gehring, Fabian Gloeckle, Sten Sootla, Itai Gat, Xiaoqing Ellen Tan, Yossi Adi, Jingyu Liu, Romain Sauvestre, Tal Remez, et al. Code llama: Open foundation models for code. *arXiv preprint arXiv:2308.12950*, 2023.
- Mingjie Sun, Zhuang Liu, Anna Bair, and J Zico Kolter. A simple and effective pruning approach for large language models. In *The Twelfth International Conference on Learning Representations*, 2024.

-
- Jiaming Tang, Yilong Zhao, Kan Zhu, Guangxuan Xiao, Baris Kasikci, and Song Han. QUEST: Query-aware sparsity for efficient long-context LLM inference. In *Forty-first International Conference on Machine Learning*, 2024.
- Rohan Taori, Ishaan Gulrajani, Tianyi Zhang, Yann Dubois, Xuechen Li, Carlos Guestrin, Percy Liang, and Tatsunori B Hashimoto. Stanford alpaca: An instruction-following llama model, 2023.
- Hugo Touvron, Thibaut Lavril, Gautier Izacard, Xavier Martinet, Marie-Anne Lachaux, Timothée Lacroix, Baptiste Rozière, Naman Goyal, Eric Hambro, Faisal Azhar, et al. Llama: Open and efficient foundation language models. *arXiv preprint arXiv:2302.13971*, 2023a.
- Hugo Touvron, Louis Martin, Kevin Stone, Peter Albert, Amjad Almahairi, Yasmine Babaei, Nikolay Bashlykov, Soumya Batra, Prajjwal Bhargava, Shruti Bhosale, et al. Llama 2: Open foundation and fine-tuned chat models. *arXiv preprint arXiv:2307.09288*, 2023b.
- Zhongwei Wan, Xinjian Wu, Yu Zhang, Yi Xin, Chaofan Tao, Zhihong Zhu, Xin Wang, Siqi Luo, Jing Xiong, Longyue Wang, and Mi Zhang. D_2O : Dynamic discriminative operations for efficient long-context inference of large language models. In *The Thirteenth International Conference on Learning Representations*, 2025.
- Thomas Wolf, Lysandre Debut, Victor Sanh, Julien Chaumond, Clement Delangue, Anthony Moi, Pierric Cistac, Tim Rault, Remi Louf, Morgan Funtowicz, et al. Transformers: State-of-the-art natural language processing. In *Proceedings of the 2020 conference on empirical methods in natural language processing: system demonstrations*, pp. 38–45, 2020.
- Guangxuan Xiao, Yuandong Tian, Beidi Chen, Song Han, and Mike Lewis. Efficient streaming language models with attention sinks. In *The Twelfth International Conference on Learning Representations*, 2024.
- Tianyi Zhang, Faisal Ladhak, Esin Durmus, Percy Liang, Kathleen McKeown, and Tatsunori B Hashimoto. Benchmarking large language models for news summarization. *Transactions of the Association for Computational Linguistics*, 12:39–57, 2024a.
- Yuxin Zhang, Yuxuan Du, Gen Luo, Yunshan Zhong, Zhenyu Zhang, Shiwei Liu, and Rongrong Ji. Cam: Cache merging for memory-efficient LLMs inference. In *Forty-first International Conference on Machine Learning*, 2024b.
- Zhenyu Zhang, Ying Sheng, Tianyi Zhou, Tianlong Chen, Lianmin Zheng, Ruisi Cai, Zhao Song, Yuandong Tian, Christopher Ré, Clark Barrett, et al. H2o: Heavy-hitter oracle for efficient generative inference of large language models. *Advances in Neural Information Processing Systems*, 36:34661–34710, 2023.

A FUTURE WORK

While effective, OBCACHE presents several opportunities for further improvement. One notable limitation is the structural bias towards earlier tokens, a common drawback in many existing cache eviction methods, which also emerges in OBCACHE, particularly as the perturbation window increase. Although heuristics like retaining a fixed-size recent window help mitigate this bias by leveraging the locality of attention patterns, such strategies remain static and empirically driven. Future work should more systematically investigate the design and adaptability of perturbation windows to better improve saliency estimation. Additionally, OBCACHE’s current dynamic cache eviction strategy in the decoding phase directly follows H₂O by accumulating saliency scores over time, effectively minimizing perturbations over the full sequence history. However, under our formulation, alternative objectives could be explored. For example, accumulating scores only within a recent attention window. Such variants may yield improved adaptability in long-context generation.

On the theoretical side, OBCACHE introduces a flexible, perturbation-minimization framework that can be extended to a broader class of KV cache compression strategies. For instance, due to the inherent flexibility of structured pruning, one could adapt the OBCACHE formulation to key channel pruning by redefining the pruning units from tokens to channels. Leveraging approximation techniques, it is possible to derive corresponding closed-form saliency scores from an output-aware perspective, enabling informed channel-level pruning decisions. Moreover, our approach relies on the diagonal Hessian assumption used in Optimal Brain Damage, which supports only token removal. In contrast, another classical pruning theory Optimal Brain Surgeon relaxes this assumption by allowing compensation across pruning units, adjusting remaining parameters to reduce loss. This perspective aligns naturally with recent works on cache merging, and could inspire more theoretically grounded cache management techniques for long-context LLMs.

Overall, OBCACHE offers a flexible foundation for future research into KV cache compression. Its structured and theoretically motivated formulation opens up promising directions for designing more effective and principled KV cache management.

B THEORETICAL ANALYSIS

In this section, we demonstrate the full proof and derivations to obtain the OBCACHE scores in Equation 5, Equation 6 and Equation 7, as well as their reduction to other attention-based scoring methods. We use consistent notations as previously defined in Section 3.1.

B.1 OBCACHE OBJECTIVE FUNCTION

As demonstrated in Section 3.2 and Section 3.4, we formulate the saliency score for a candidate key-value token as Equation 2, which is the *pruning-induced eviction error* within a *perturbation window* for query positions w through s :

$$\mathcal{L}(\widehat{\mathbf{V}}, \widehat{\mathbf{K}}) := \|\widehat{\mathbf{O}}_{w:s} - \mathbf{O}_{w:s}\|_F^2 = \|\text{softmax}(\frac{\mathbf{Q}_{w:s}\widehat{\mathbf{K}}^\top}{\sqrt{d}})\widehat{\mathbf{V}} - \text{softmax}(\frac{\mathbf{Q}_{w:s}\mathbf{K}^\top}{\sqrt{d}})\mathbf{V}\|_F^2. \quad (11)$$

In what follows, we let $\mathbf{O}_{i,j} = \mathbf{a}_i \mathbf{V}_{:,j}$ denote the j -th feature element in the i -th row vector of the attention output matrix \mathbf{O} , where \mathbf{a}_i is the i -th row vector of the attention weight matrix. The squared Frobenius norm objective in Equation 11 can be explicitly decomposed into a summation form across all element-wise squared error:

$$\begin{aligned} \mathcal{L}(\widehat{\mathbf{V}}, \widehat{\mathbf{K}}) &= \sum_{i=w}^s \sum_{j=1}^d |\widehat{\mathbf{O}}_{i,j} - \mathbf{O}_{i,j}|^2 \\ &= \sum_{i=w}^s \sum_{j=1}^d |\text{softmax}(\frac{\mathbf{a}_i \widehat{\mathbf{K}}^\top}{\sqrt{d}})\widehat{\mathbf{V}}_{:,j} - \text{softmax}(\frac{\mathbf{a}_i \mathbf{K}^\top}{\sqrt{d}})\mathbf{V}_{:,j}|^2 \\ &\triangleq \sum_{i=w}^s \sum_{j=1}^d \mathbf{E}_{i,j}. \end{aligned} \quad (12)$$

For clarity in the following derivations, we define $\mathbf{E}_{i,j} := |\widehat{\mathbf{O}}_{i,j} - \mathbf{O}_{i,j}|^2$ as the squared difference of the output element $\mathbf{O}_{i,j}$ before and after applying a perturbation $\delta\mathbf{V}$ and $\delta\mathbf{K}$. Expanding explicitly, the *element-wise output perturbation* for $\mathbf{O}_{i,j}$ is:

$$\mathbf{E}_{i,j}(\widehat{\mathbf{V}}_{:,j}, \widehat{\mathbf{K}}) = |\text{softmax}(\frac{\mathbf{q}_i \widehat{\mathbf{K}}^\top}{\sqrt{d}}) \widehat{\mathbf{V}}_{:,j} - \text{softmax}(\frac{\mathbf{q}_i \mathbf{K}^\top}{\sqrt{d}}) \mathbf{V}_{:,j}|^2. \quad (13)$$

Given this element-wise objective, we follow the Optimal Brain Damage (OBD) theory (LeCun et al., 1989) to apply a second-order Taylor expansion of $\mathbf{E}_{i,j}$ around $(\mathbf{V}_{:,j}, \mathbf{K})$, and analytically approximate the element-wise output perturbation:

$$\begin{aligned} \mathbf{E}_{i,j}(\widehat{\mathbf{V}}_{:,j}, \widehat{\mathbf{K}}) \stackrel{\text{second}}{\approx} \mathbf{E}_{i,j}(\mathbf{V}_{:,j}, \mathbf{K}) &+ \delta\mathbf{V}_{:,j}^\top \frac{\partial \mathbf{E}_{i,j}(\mathbf{V}_{:,j}, \mathbf{K})}{\partial \widehat{\mathbf{V}}_{:,j}} + \frac{1}{2} \delta\mathbf{V}_{:,j}^\top \frac{\partial^2 \mathbf{E}_{i,j}(\mathbf{V}_{:,j}, \mathbf{K})}{\partial \widehat{\mathbf{V}}_{:,j}^2} \delta\mathbf{V}_{:,j} \\ &+ \delta\mathbf{K}^\top \frac{\partial \mathbf{E}_{i,j}(\mathbf{V}_{:,j}, \mathbf{K})}{\partial \widehat{\mathbf{K}}} + \frac{1}{2} \delta\mathbf{K}^\top \frac{\partial^2 \mathbf{E}_{i,j}(\mathbf{V}_{:,j}, \mathbf{K})}{\partial \widehat{\mathbf{K}}^2} \delta\mathbf{K} \\ &+ \delta\mathbf{V}_{:,j}^\top \frac{\partial^2 \mathbf{E}_{i,j}(\mathbf{V}_{:,j}, \mathbf{K})}{\partial \widehat{\mathbf{V}}_{:,j} \partial \widehat{\mathbf{K}}} \delta\mathbf{K} + \mathcal{O}(\|(\delta\mathbf{V}_{:,j}, \delta\mathbf{K})\|^3). \end{aligned}$$

Through substitution into Equation 13, the constant term $\mathbf{E}_{i,j}(\mathbf{V}_{:,j}, \mathbf{K})$ vanishes because we have $\widehat{\mathbf{O}}_{i,j} - \mathbf{O}_{i,j} = 0$ at the expansion point $(\mathbf{V}_{:,j}, \mathbf{K})$. Therefore, the full matrix-wise objective, *pruning-induced eviction error*, approximated via a Taylor-series to the second order, becomes:

$$\mathcal{L}(\widehat{\mathbf{V}}, \widehat{\mathbf{K}}) \stackrel{\text{second}}{\approx} \sum_{i=w}^s \sum_{j=1}^d \delta\mathbf{V}_{:,j}^\top \frac{\partial \mathbf{E}_{i,j}(\mathbf{V}_{:,j}, \mathbf{K})}{\partial \widehat{\mathbf{V}}_{:,j}} + \frac{1}{2} \delta\mathbf{V}_{:,j}^\top \frac{\partial^2 \mathbf{E}_{i,j}(\mathbf{V}_{:,j}, \mathbf{K})}{\partial \widehat{\mathbf{V}}_{:,j}^2} \delta\mathbf{V}_{:,j} \quad (14)$$

$$\sum_{i=w}^s \sum_{j=1}^d \delta\mathbf{K}^\top \frac{\partial \mathbf{E}_{i,j}(\mathbf{V}_{:,j}, \mathbf{K})}{\partial \widehat{\mathbf{K}}} + \frac{1}{2} \delta\mathbf{K}^\top \frac{\partial^2 \mathbf{E}_{i,j}(\mathbf{V}_{:,j}, \mathbf{K})}{\partial \widehat{\mathbf{K}}^2} \delta\mathbf{K} \quad (15)$$

$$\sum_{i=w}^s \sum_{j=1}^d \delta\mathbf{V}_{:,j}^\top \frac{\partial^2 \mathbf{E}_{i,j}(\mathbf{V}_{:,j}, \mathbf{K})}{\partial \widehat{\mathbf{V}}_{:,j} \partial \widehat{\mathbf{K}}} \delta\mathbf{K}. \quad (16)$$

B.2 ISOLATED VALUE-PRUNING SCORE

In isolated value pruning, the key-cache matrix is not perturbed and is considered a constant not affecting \mathcal{L} . Therefore, minimizing the pruning-induced eviction error reduces to minimizing Equation 14. To derive saliency scores in closed form, we begin by deriving expressions for the gradient and Hessian with respect to $\widehat{\mathbf{V}}_{:,j}$. The first-order derivative of $\mathbf{E}_{i,j}$ with respect to $\widehat{\mathbf{V}}_{:,j}$ is:

$$\frac{\partial \mathbf{E}_{i,j}}{\partial \widehat{\mathbf{V}}_{:,j}} = \frac{\partial}{\partial \widehat{\mathbf{V}}_{:,j}} |\widehat{\mathbf{O}}_{i,j} - \mathbf{O}_{i,j}|^2 = 2(\widehat{\mathbf{O}}_{i,j} - \mathbf{O}_{i,j}) \frac{\partial}{\partial \widehat{\mathbf{V}}_{:,j}} \widehat{\mathbf{a}}_i \widehat{\mathbf{V}}_{:,j} = 2(\widehat{\mathbf{O}}_{i,j} - \mathbf{O}_{i,j}) \widehat{\mathbf{a}}_i. \quad (17)$$

When evaluated at $(\mathbf{V}_{:,j}, \mathbf{K})$, we again have $\widehat{\mathbf{O}}_{i,j} - \mathbf{O}_{i,j} = 0$, so the gradient term vanishes to zero. The Hessian of \mathcal{L} with respect to $\widehat{\mathbf{V}}_{:,j}$ evaluated at $(\mathbf{V}_{:,j}, \mathbf{K})$ is:

$$\frac{\partial^2 \mathbf{E}_{i,j}(\mathbf{V}_{:,j}, \mathbf{K})}{\partial \widehat{\mathbf{V}}_{:,j}^2} = 2 \frac{\partial}{\partial \widehat{\mathbf{O}}_{i,j}} \left((\widehat{\mathbf{O}}_{i,j} - \mathbf{O}_{i,j}) \widehat{\mathbf{a}}_i^\top \right) \left(\frac{\partial \widehat{\mathbf{O}}_{i,j}}{\partial \widehat{\mathbf{V}}_{:,j}} \right)^\top \Bigg|_{(\mathbf{V}_{:,j}, \mathbf{K})} = 2 \mathbf{a}_i^\top \mathbf{a}_i. \quad (18)$$

Substituting the gradient and Hessian back into Equation 14, we get the pruning-induced eviction error when value states are considered as isolate pruning units:

$$\mathcal{L}^{\text{value}} = \sum_{i=w}^s \sum_{j=1}^d \delta\mathbf{V}_{:,j}^\top (\mathbf{a}_i^\top \mathbf{a}_i) \delta\mathbf{V}_{:,j} = \sum_{i=w}^s \sum_{j=1}^d |\mathbf{a}_i \delta\mathbf{V}_{:,j}|^2. \quad (19)$$

Next, the row-wise pruning constraint in Equation 1 implies that when pruning the p -th token position, the value cache perturbation $\delta\mathbf{V}_{:,j}$ is explicitly in the form:

$$\delta\mathbf{V}_{t,j} = \begin{cases} -\mathbf{V}_{p,j}, & \text{when } t = p \\ 0, & \text{when } t \neq p \end{cases}, \quad \forall j = 1, \dots, d.$$

Substituting this value perturbation into $\mathcal{L}^{\text{value}}$, we obtain the output perturbation when pruning the p -th value vector from the value cache \mathbf{V} :

$$S_p^{\text{value}} = \sum_{i=w}^s \sum_{j=1}^d |\mathbf{A}_{i,p} \cdot \mathbf{V}_{p,j}|^2 = \sum_{i=w}^s |\mathbf{A}_{i,p}|^2 \cdot \sum_{j=1}^d |\mathbf{V}_{p,j}|^2 = \boxed{\sum_{i=w}^s |\mathbf{A}_{i,p}|^2 \cdot \|\mathbf{v}_p\|^2}. \quad (20)$$

This is also the value-pruning saliency score for evicting the p -th value vector \mathbf{v}_p from the value cache. It is consistent with the expression in Equation 5 in Section 3.3.

B.3 ISOLATED KEY-PRUNING SCORE

In isolated key pruning, the value-cache matrix is not perturbed and is assumed a constant. Therefore, minimizing the pruning-induced eviction error reduces to minimizing Equation 15. Same as in value-pruning score, we begin by deriving closed-form expressions for the gradient and Hessian with respect to $\widehat{\mathbf{K}}$. The first-order derivative of $E_{i,j}$ with respect to $\widehat{\mathbf{K}}$ is:

$$\frac{\partial E_{i,j}}{\partial \widehat{\mathbf{K}}} = \frac{\partial}{\partial \widehat{\mathbf{K}}} |\widehat{\mathbf{O}}_{i,j} - \mathbf{O}_{i,j}|^2 = 2(\widehat{\mathbf{O}}_{i,j} - \mathbf{O}_{i,j}) \frac{\partial \widehat{\mathbf{O}}_{i,j}}{\partial \widehat{\mathbf{K}}}. \quad (21)$$

Before deriving the first-order term explicitly, note that when evaluated at the point $(\mathbf{V}_{:,j}, \mathbf{K})$, we again have $\widehat{\mathbf{O}}_{i,j} - \mathbf{O}_{i,j} = 0$. Consequently, the first-order term is eliminated, a result that is the same as in isolated value pruning. We now explicitly derive the term $\widehat{M}^{(i,j)} := \frac{\partial \widehat{\mathbf{O}}_{i,j}}{\partial \widehat{\mathbf{K}}}$ above:

$$\begin{aligned} \widehat{M}_{p,r}^{(i,j)} &= \left(\frac{\partial \widehat{\mathbf{O}}_{i,j}}{\partial \widehat{\mathbf{K}}} \right)_{p,r} = \frac{\partial}{\partial \widehat{\mathbf{K}}_{p,r}} \sum_{m=1}^s \widehat{\mathbf{A}}_{i,m} \cdot \widehat{\mathbf{V}}_{m,j} = \sum_{m=1}^s \frac{\partial \widehat{\mathbf{O}}_{i,j}}{\partial \widehat{\mathbf{A}}_{i,m}} \frac{\partial \widehat{\mathbf{A}}_{i,m}}{\partial \widehat{\mathbf{K}}_{p,r}} \\ &= \sum_{m=1}^s \frac{\partial \widehat{\mathbf{O}}_{i,j}}{\partial \widehat{\mathbf{A}}_{i,m}} \frac{\partial}{\partial \widehat{\mathbf{K}}_{p,r}} \left(\frac{e^{\widehat{\mathbf{Z}}_{i,m}}}{\sum_{u=1}^s e^{\widehat{\mathbf{Z}}_{i,u}}} \right) \\ &= \sum_{m=1}^s \frac{\partial \widehat{\mathbf{O}}_{i,j}}{\partial \widehat{\mathbf{A}}_{i,m}} \sum_{u=1}^s \frac{\widehat{\mathbf{A}}_{i,m} \cdot \widehat{\mathbf{Z}}_{i,u}}{\widehat{\mathbf{Z}}_{i,u}} \frac{\partial \widehat{\mathbf{Z}}_{i,u}}{\partial \widehat{\mathbf{K}}_{p,r}} \\ &= \sum_{m=1}^s \widehat{\mathbf{V}}_{m,j} \sum_{u=1}^s \widehat{\mathbf{A}}_{i,m} (\delta_{mu} - \widehat{\mathbf{A}}_{i,u}) \frac{1}{\sqrt{d}} \mathbf{Q}_{i,r} \delta_{up} \\ &= \sum_{m=1}^s \widehat{\mathbf{V}}_{m,j} \cdot \widehat{\mathbf{A}}_{i,m} (\delta_{mp} - \widehat{\mathbf{A}}_{i,p}) \frac{1}{\sqrt{d}} \mathbf{Q}_{i,r} \quad (\delta_{up} = 0 \text{ when } u \neq p) \\ &= \frac{1}{\sqrt{d}} \mathbf{Q}_{i,r} \cdot \left(\sum_{m=1}^s \widehat{\mathbf{V}}_{m,j} \cdot \widehat{\mathbf{A}}_{i,m} \cdot \delta_{mp} - \sum_{m=1}^s \widehat{\mathbf{V}}_{m,j} \cdot \widehat{\mathbf{A}}_{i,m} \cdot \widehat{\mathbf{A}}_{i,p} \right) \\ &= \frac{1}{\sqrt{d}} \mathbf{Q}_{i,r} \cdot (\widehat{\mathbf{V}}_{p,j} \cdot \widehat{\mathbf{A}}_{i,p} - \widehat{\mathbf{A}}_{i,p} \cdot \sum_{m=1}^s \widehat{\mathbf{V}}_{m,j} \cdot \widehat{\mathbf{A}}_{i,m}) \quad (\delta_{mp} = 0 \text{ when } m \neq p) \\ &= \frac{1}{\sqrt{d}} \mathbf{Q}_{i,r} \cdot \widehat{\mathbf{A}}_{i,p} \cdot (\widehat{\mathbf{V}}_{p,j} - \widehat{\mathbf{O}}_{i,j}). \end{aligned} \quad (22)$$

Therefore, the first-order derivative of $E_{i,j}$ with respect to the perturbed key cache $\widehat{\mathbf{K}}$ is:

$$\frac{\partial E_{i,j}}{\partial \widehat{\mathbf{K}}} = 2(\widehat{\mathbf{O}}_{i,j} - \mathbf{O}_{i,j}) \widehat{M}^{(i,j)}, \text{ where } \widehat{M}_{p,r}^{(i,j)} = \frac{1}{\sqrt{d}} \mathbf{Q}_{i,r} \cdot \widehat{\mathbf{A}}_{i,p} \cdot (\widehat{\mathbf{V}}_{p,j} - \widehat{\mathbf{O}}_{i,j}).$$

We now proceed to derive the Hessian, which is a 4-th order tensor of size $s \times d \times s \times d$. The second-order derivative of the element-wise perturbation $E_{i,j}$ with respect to $\widehat{\mathbf{K}}$ is:

$$\begin{aligned} \frac{\partial E_{i,j}}{\partial \widehat{\mathbf{K}}^2} &= \widehat{M}^{(i,j)} \otimes \left(\frac{\partial}{\partial \widehat{\mathbf{K}}} 2(\widehat{\mathbf{O}}_{i,j} - \mathbf{O}_{i,j}) \right) + 2(\widehat{\mathbf{O}}_{i,j} - \mathbf{O}_{i,j}) \frac{\partial \widehat{M}^{(i,j)}}{\partial \widehat{\mathbf{K}}} \\ &= \widehat{M}^{(i,j)} \otimes \widehat{M}^{(i,j)} + 2(\widehat{\mathbf{O}}_{i,j} - \mathbf{O}_{i,j}) \frac{\partial \widehat{M}^{(i,j)}}{\partial \widehat{\mathbf{K}}}, \end{aligned} \quad (23)$$

where \otimes denotes the matrix-wise outer product¹. Since the Hessian will be evaluated at the point $(\mathbf{V}_{:,j}, \mathbf{K})$, where the perturbed attention output again matches the original, i.e., $\widehat{\mathbf{O}}_{i,j} - \mathbf{O}_{i,j} = 0$, the second term in Equation 23 vanishes. Therefore, the Hessian is:

$$\frac{\partial^2 \mathbf{E}_{i,j}}{\partial \widehat{\mathbf{K}}^2} \Big|_{(\mathbf{v}_{:,j}, \mathbf{K})} = 2\mathbf{M}^{(i,j)} \otimes \mathbf{M}^{(i,j)} = 2\text{vec}(\mathbf{M}^{(i,j)})^\top \text{vec}(\mathbf{M}^{(i,j)}), \quad (24)$$

$$\text{where } \mathbf{M}_{p,r}^{(i,j)} = \frac{1}{\sqrt{d}} \mathbf{Q}_{i,r} \cdot \mathbf{A}_{i,p} \cdot (\mathbf{V}_{p,j} - \mathbf{O}_{i,j}).$$

Here, we use $\text{vec}(\cdot)$ to denote the vectorization of a matrix. Substituting the gradient and Hessian back into Equation 15, we get the pruning-induced eviction error when key states are considered as isolate pruning units:

$$\begin{aligned} \mathcal{L}^{\text{key}} &= \sum_{i=w}^s \sum_{j=1}^d \text{vec}(\delta \mathbf{K})^\top \text{vec}(\mathbf{M}^{(i,j)})^\top \text{vec}(\mathbf{M}^{(i,j)}) \text{vec}(\delta \mathbf{K}) \\ &= \sum_{i=w}^s \sum_{j=1}^d |\text{vec}(\mathbf{M}^{(i,j)}) \text{vec}(\delta \mathbf{K})|^2. \end{aligned} \quad (25)$$

Similarly, the row-wise pruning constraint in Equation 1 implies that when pruning the p -th token position, the key cache perturbation $\delta \mathbf{K}$ is explicitly in the form:

$$\delta \mathbf{K}_{t,j} = \begin{cases} -\mathbf{K}_{p,j}, & \text{when } t = p, \\ 0, & \text{when } t \neq p, \end{cases} \quad \forall j = 1, \dots, d.$$

Substituting this key perturbation into \mathcal{L}^{key} , we obtain the output perturbation when pruning the p -th value vector from the value cache \mathbf{K} (we let $\mathbf{m}_p^{(i,j)}$ to denote the p -th row vector of $\mathbf{M}^{(i,j)}$):

$$\begin{aligned} \mathbf{S}_p^{\text{key}} &= \sum_{i=w}^s \sum_{j=1}^d |\mathbf{m}_p^{(i,j)} \mathbf{k}_p|^2 = \sum_{i=w}^s \sum_{j=1}^d \left| \sum_{r=1}^d \frac{1}{\sqrt{d}} \mathbf{Q}_{i,r} \cdot \mathbf{A}_{i,p} (\mathbf{V}_{p,j} - \mathbf{O}_{i,j}) \cdot \mathbf{K}_{p,r} \right|^2 \\ &= \frac{1}{d} \sum_{i=w}^s \sum_{j=1}^d \left| \mathbf{A}_{i,p} (\mathbf{V}_{p,j} - \mathbf{O}_{i,j}) \cdot \sum_{r=1}^d \mathbf{Q}_{i,r} \mathbf{K}_{p,r} \right|^2 \\ &= \frac{1}{d} \sum_{i=w}^s \sum_{j=1}^d \left| \mathbf{A}_{i,p} (\mathbf{V}_{p,j} - \mathbf{O}_{i,j}) \cdot \mathbf{q}_i \mathbf{k}_p^\top \right|^2 \\ &= \frac{1}{d} \sum_{i=w}^s \left(\left| \mathbf{A}_{i,p} \right|^2 \cdot \left| \mathbf{q}_i \mathbf{k}_p^\top \right|^2 \sum_{j=1}^d \left| \mathbf{V}_{p,j} - \mathbf{O}_{i,j} \right|^2 \right) \\ &= \boxed{\sum_{i=w}^s \left| \mathbf{A}_{i,p} \right|^2 \cdot \left| \mathbf{Z}_{i,p} \right|^2 \cdot \left\| \mathbf{v}_p - \mathbf{o}_i \right\|_2^2}. \end{aligned}$$

This is also the key-pruning saliency score for evicting the p -th key vector \mathbf{k}_p from the key cache. It is consistent with the expression in Equation 6 in Section 3.3.

B.4 JOINT-PRUNING SCORE

When both $\mathbf{V}_{:,j}$ and \mathbf{K} are treated as variables affecting \mathcal{L} , we need to compute the cross-term in the error function, which corresponds to deriving a closed-form expression for Equation 16. Given that the first-order derivative of $\mathbf{E}_{i,j}$ with respect to $\widehat{\mathbf{V}}_{:,j}$ is known, we can compute the cross-term as follows:

$$\begin{aligned} \frac{\partial^2 \mathbf{E}_{i,j}}{\partial \widehat{\mathbf{V}}_{:,j} \partial \widehat{\mathbf{K}}} &= \frac{\partial}{\partial \widehat{\mathbf{K}}} 2(\widehat{\mathbf{O}}_{i,j} - \mathbf{O}_{i,j}) \widehat{\mathbf{a}}_i \\ &= \widehat{\mathbf{a}}_i \otimes \left(\frac{\partial}{\partial \widehat{\mathbf{K}}} 2(\widehat{\mathbf{O}}_{i,j} - \mathbf{O}_{i,j}) \right) + 2(\widehat{\mathbf{O}}_{i,j} - \mathbf{O}_{i,j}) \frac{\partial \widehat{\mathbf{a}}_i}{\partial \widehat{\mathbf{K}}}. \end{aligned} \quad (26)$$

¹For any two matrices $\mathbf{C}, \mathbf{D} \in \mathbb{R}^{s \times d}$, the output tensor via outer product is $\mathbf{C} \otimes \mathbf{D} \in \mathbb{R}^{s \times d \times s \times d}$.

Same as in deriving key-pruning scores, the second term above will be zero when evaluated at the point $(\mathbf{V}_{:,j}, \mathbf{K})$. Therefore, the cross second-order term is:

$$\left. \frac{\partial^2 \mathbf{E}_{i,j}}{\partial \widehat{\mathbf{V}}_{:,j} \partial \widehat{\mathbf{K}}} \right|_{(\mathbf{v}_{:,j}, \mathbf{K})} = 2\mathbf{a}_i \otimes M^{(i,j)}, \text{ where } M_{p,r}^{(i,j)} = \frac{1}{\sqrt{d}} \mathbf{Q}_{i,r} \cdot \mathbf{A}_{i,p} \cdot (\mathbf{V}_{p,j} - \mathbf{O}_{i,j}). \quad (27)$$

Substituting this back into Equation 16, we get the cross-term of the pruning-induced eviction error when the value and key states are considered as combined pruning units:

$$\mathcal{L}^{\text{cross}} = \sum_{i=w}^s \sum_{j=1}^d \delta \mathbf{V}_{:,j}^\top (2\mathbf{a}_i \otimes M^{(i,j)}) \delta \mathbf{K} = 2 \sum_{i=w}^s \sum_{j=1}^d (\delta \mathbf{V}_{:,j}^\top \mathbf{a}_i) \cdot \langle M^{(i,j)}, \delta \mathbf{K} \rangle_F, \quad (28)$$

where $\langle M^{(i,j)}, \delta \mathbf{K} \rangle_F = \sum_{p,r} M_{p,r}^{(i,j)} \cdot \delta \mathbf{K}_{p,r} = \text{tr}(M^{(i,j)\top} \delta \mathbf{K})$ is the Frobenius inner product.

When the p -th key and value are pruned, the row-wise pruning constraint in Equation 1 implies that the value cache perturbation $\delta \mathbf{V}$ and the key cache perturbation $\delta \mathbf{K}$ are explicitly in the form:

$$\delta \mathbf{V}_{t,j} = \begin{cases} -\mathbf{V}_{p,j}, & \text{when } t = p \\ 0, & \text{when } t \neq p \end{cases}, \quad \delta \mathbf{K}_{t,j} = \begin{cases} -\mathbf{K}_{p,j}, & \text{when } t = p \\ 0, & \text{when } t \neq p \end{cases}, \quad \forall j = 1, \dots, d.$$

Thus, we have each term in $\mathcal{L}^{\text{cross}}$:

$$\delta \mathbf{V}_{:,j}^\top \mathbf{a}_i = -\mathbf{A}_{i,p} \mathbf{V}_{p,j}, \quad \langle M^{(i,j)}, \delta \mathbf{K} \rangle_F = -\frac{1}{\sqrt{d}} \mathbf{A}_{i,p} \cdot (\mathbf{V}_{p,j} - \mathbf{O}_{i,j}) \cdot (\mathbf{q}_i \mathbf{k}_p^\top).$$

Substituting these two expressions back into Equation 28, we obtain the cross term in closed form:

$$\begin{aligned} \mathcal{L}^{\text{cross}} &= \frac{2}{\sqrt{d}} \sum_{i=w}^s \sum_{j=1}^d \mathbf{A}_{i,p}^2 \cdot \mathbf{V}_{p,j} \cdot (\mathbf{V}_{p,j} - \mathbf{O}_{i,j}) \cdot (\mathbf{q}_i \mathbf{k}_p^\top) \\ &= \frac{2}{\sqrt{d}} \sum_{i=w}^s \mathbf{A}_{i,p}^2 \cdot (\mathbf{q}_i \mathbf{k}_p^\top) \sum_{j=1}^d \mathbf{V}_{p,j} (\mathbf{V}_{p,j} - \mathbf{O}_{i,j}) \\ &= \boxed{2 \sum_{i=w}^s \mathbf{A}_{i,p}^2 \cdot \mathbf{Z}_{i,p} \cdot (\|\mathbf{v}_p\|_2^2 - \mathbf{v}_p^\top \mathbf{o}_i)}. \end{aligned} \quad (29)$$

Finally, the saliency score of the token at position p when both value and key states are treated as pruning units is the summation of $\mathcal{L}^{\text{value}}$, \mathcal{L}^{key} and $\mathcal{L}^{\text{cross}}$:

$$\boxed{\mathcal{S}_p^{\text{joint}} = 2 \sum_{i=w}^s \mathbf{A}_{i,p}^2 \cdot \mathbf{Z}_{i,p} \cdot (\|\mathbf{v}_p\|_2^2 - \mathbf{v}_p^\top \mathbf{o}_i) + \mathcal{S}_p^{\text{value}} + \mathcal{S}_p^{\text{key}}}. \quad (30)$$

This is consistent with the joint score expression in Equation 7 of Section 3.3.

B.5 REDUCTION TO ATTENTION-BASED SCORES

We now show in detail that existing attention-based scores can be naturally recovered within our pruning framework. Suppose the pruning objective is defined over perturbations in the historical attention weights, $\mathbf{A}_{w:s}$, rather than in the attention outputs, $\mathbf{O}_{w:s}$. Further, assume that each pruning unit corresponds to a single column of the attention matrix. Under these assumptions, minimizing the pruning-induced eviction error reduces to the following optimization problem:

$$\arg \min_p \|\widehat{\mathbf{A}}_{w:s} - \mathbf{A}_{w:s}\|_{1,1} \quad \text{s.t.} \quad \delta \mathbf{A}_{w:s} \mathbf{e}_p + \mathbf{A}_{w:s,p} = \mathbf{0},$$

where $\|\cdot\|_{1,1}$ denotes the entry-wise matrix L_1 norm. In this case, the pruning constraint can be directly substituted into the objective, yielding the saliency score for token position p :

$$\boxed{\mathcal{S}_p^{\text{attn-based}} = \|\mathbf{A}_{w:s,p}\|_{1,1} = \sum_{i=w}^s |\mathbf{A}_{i,p}|}. \quad (31)$$

This represents the L_1 -norm variant of our value-pruning score, $\mathcal{S}_p^{\text{value}}$, but it excludes any value-state information. By varying the choice of the window index w , the score $\mathcal{S}_p^{\text{attn-based}}$ can flexibly target different perturbation windows, corresponding to various existing attention-based cache eviction strategies such as H₂O, TOVA, and SnapKV.

C EXPERIMENTAL SETUP

All the experiments are conducted on a single NVIDIA A100 GPU. We adapt the Hugging Face Transformers library (Wolf et al., 2020) with PyTorch (Paszke et al., 2019) to implement the cache eviction algorithms. We use two representative instruction-tuned large language models as backbones: LLaMA-3.1-8B-Instruct (Grattafiori et al., 2024) and Qwen-2.5-7B-Instruct (Bai et al., 2023a). Both models employ Grouped Query Attention (GQA) and natively support a context window size of up to 128K tokens. All model inference is performed in half precision (bfloat16) with no quantization applied.

For tasks with extensive prefill prompt lengths, we use FlashAttention-2 (Dao, 2023) for prefill attention computation to reduce memory overhead. We then recompute attention weights for selected query positions as needed to compute saliency scores for token eviction, since attention weights are not materialized in FlashAttention.

C.1 DATASETS

We evaluate OBCACHE and existing cache eviction methods on three benchmarks: Needle-In-A-Haystack (Kamradt, 2023), LongBench (Bai et al., 2023b), and perplexity on the PG19 dataset (Rae et al., 2019), targeting prefill-phase static cache eviction and decoding-phase dynamic cache eviction, respectively.

Needle-In-A-Haystack (NIAH). We follow the setup from the RULER benchmark (Hsieh et al., 2024), specifically the `niah_single_2` task², where a randomly generated 7-digit “needle” passkey is embedded into a Paul Graham essay haystack. Context lengths of 4K, 8K, 16K, and 32K tokens are tested, with each setting containing 250 randomly generated samples.

LongBench. LongBench includes 16 datasets across six task categories: single-document QA, multi-document QA, summarization, few-shot learning, synthetic reasoning, and code completion. The average input length is 6,711 words (approximately 16K tokens). For all models and methods, we truncate each sample to a maximum of 32K tokens. To ensure fair comparison, we follow SnapKV (Li et al., 2024) and perform cache eviction only during the prefill phase. Task-specific evaluation metrics (e.g., Exact Match/F1 for QA tasks, ROUGE for summarization tasks) are reported using LongBench’s official evaluation script³.

Perplexity. For decoding-phase cache eviction, we adopt the PG19 test set following the setup in StreamingLLM (Xiao et al., 2024). PG19 contains 100 full-length books, each averaging around 70K tokens. We evaluate on the standard test split⁴ and compute perplexity across varying context lengths (from 1 to 32K), using a fixed KV cache budget of 1024 tokens for all dynamic cache eviction methods.

C.2 BASELINE SETUPS

C.2.1 PREFILL EVICTION

To evaluate baselines for prefill-phase cache eviction, we follow the experimental setup of SnapKV (Li et al., 2024) and perform cache eviction only during the prefill phase. Since SnapKV does not support eviction during decoding, no cached tokens are evicted in the decoding phase (for NIAH and LongBench tasks). In these benchmarks, the prompt length dominates and is the primary bottleneck; thus, applying decoding-phase eviction has little impact on performance.

H₂O. H₂O originally accumulates attention weights across all historical query positions to make eviction decisions. This is incompatible with the FlashAttention prefill implementation, as it requires recomputing full attention weights. To enable efficient implementation, we follow SnapKV’s version of H₂O and accumulate query positions only within a recent perturbation window. For NIAH tasks,

²<https://github.com/NVIDIA/RULER/blob/main/README.md>

³<https://github.com/THUDM/LongBench/blob/main/LongBench/pred.py>

⁴<https://huggingface.co/datasets/emozilla/pg19>

the perturbation window size is set to 16. For LongBench tasks, the window size is 5% of the prompt length l . All tokens in the perturbation window are treated as recent tokens, and the remaining cache budget is allocated to select heavy hitters.

TOVA. TOVA does not accumulate attention weights but makes eviction decisions solely based on the most recent attention distribution. In all prefill-eviction evaluations, the cache budget is entirely allocated to the heavy hitters.

SnapKV. In SnapKV, the same perturbation window as in H₂O is used. The key difference is that SnapKV additionally applies a max-pooling filter to the accumulated scores before eviction. For all SnapKV and OBCACHE-enhanced experiments, we follow the official implementation, using a max-pooling function with a kernel size of 7 and a stride of 1.

C.2.2 DECODING EVICTION

To evaluate baselines for decoding-phase cache eviction, we follow the setup of StreamingLLM (Xiao et al., 2024), where eviction decisions are made at every decoding step. All eviction methods are evaluated with a fixed 1024-token cache budget.

StreamingLLM. For StreamingLLM, we maintain the first 4 tokens as attention sinks and always keep the most recent 1020 tokens. Since attention sinks are essential for long-context generation, we retain the first 4 sink tokens in all other methods as well.

H₂O. At each decoding step, H₂O accumulates attention weights across all historical query positions to make eviction decisions. In all perplexity experiments of H₂O and its OBCACHE-enhanced variants, a 256-token recent window is always reserved. The remaining 764 tokens are dynamically selected using their respective saliency scores.

TOVA. As in prefill eviction, TOVA does not use a fixed recent window. All 1020 heavy-hitter tokens are dynamically selected based on the attention scores from the latest query position.

D IMPLEMENTATION OF OBCACHE

We provide a code implementation of OBCACHE in pseudo PyTorch style, as illustrated in Algorithm 1 and Algorithm 2. These two algorithms demonstrate the computation of OBCACHE saliency scores and the cache eviction operation in the prefill phase.

E EXPERIMENTAL RESULTS

E.1 LONGBENCH FULL TABLES

Due to space constraints, we present the full table results of LongBench in Table 2 and Table 3.

Algorithm 1 Implementation of OBCACHE score update in pseudo PyTorch style.

```
1 # key_states/value_states: cache matrix (bsz, num_heads, kv_len, head_dim);
2 # A/Z: attention weight/logit matrix (bsz, num_heads, q_len, kv_len);
3 # O: attention output matrix (bsz, num_heads, q_len, head_dim);
4 # w: perturbation window start index;
5
6 def obcache_score(key_states, value_states, A, Z, O, w):
7     # Target only the perturbation window
8     A = A[..., -w:, :]
9     Z = Z[..., -w:, :]
10    O = O[..., -w:, :]
11
12    # Compute accumulated attention-based score
13    S_attn_based = A.pow(2).sum(-2)
14    ### Existing cache eviction scores (e.g., H2O and TOVA) end here ###
15
16    # Compute value-pruning score
17    V_2norm = value_states.pow(2).sum(dim=-1)
18    S_value = S_attn * V_2norm
19
20    # Compute key-pruning score
21    O_2norm = O.pow(2).sum(dim=-1)
22    VO = torch.einsum('bhqd,bhpd->bhqp', O, V)
23    VmO_2norm = O_2norm.unsqueeze(-1) + V_2norm.unsqueeze(-2) - 2 * VO
24    S_key = ((A * Z).pow(2) * VmO_2norm).sum(dim=-2)
25
26    # Compute joint-pruning score
27    VVmO = V_2norm.unsqueeze(-2) - VO
28    S_joint = (2 * A.pow(2) * Z * VVmO).sum(dim=-2) + S_value + S_key
29
30    return S_attn_based, S_value, S_key, S_joint
```

Algorithm 2 Implementation of OBCACHE cache eviction in pseudo PyTorch style.

```
1 # S: cache eviction saliency score matrix (bsz, num_heads, kv_len);
2 # num_hh / num_recent: cache budget allocated for recent and heavy-hitter tokens;
3 # num_coming: number of maximum tokens to come in next step;
4
5 def evict_kv(S, key_states, value_states, num_hh, num_recent, num_coming):
6     bsz, num_heads, kv_len, head_dim = value_states.shape
7     cutoff = kv_len - num_recent + num_coming
8
9     # Select most salient token positions
10    keep_topk_idx = torch.topk(S[..., :cutoff], num_hh, dim=-1)[1].sort().values
11    keep_topk_idx = keep_topk_idx.unsqueeze(-1).expand(-1, -1, -1, head_dim)
12
13    # Evict and keep recent
14    k_hh = torch.gather(key_states[..., :cutoff, :], dim=-2, index=keep_topk_idx)
15    k_compress = torch.cat([k_hh, key_states[..., cutoff:, :]], dim=-2)
16
17    v_hh = torch.gather(value_states[..., :cutoff, :], dim=-2, index=keep_topk_idx)
18    v_compress = torch.cat([v_hh, value_states[..., cutoff:, :]], dim=-2)
19
20    return k_compress, v_compress
```

Table 2: LongBench results for LLaMA-3.1-8B-Instruct.

Methods	Single-Document QA			Multi-Document QA			Summarization			Few-shot Learning			Synthetic		Code		
	NrvQA	Qasper	MF-en	HotpotQA	2WikiMQA	Musique	GovReport	QMSum	MultiNews	TREC	TriviaQA	SAMSum	PCount	Pre	Lec	RB-P	
ALL KV	28.79	44.75	55.21	55.53	45.59	30.89	35.01	25.39	27.23	72.5	91.65	43.75	6.78	99.5	52.23	49.39	
5% KV	H2O	24.81	30.09	47.46	52.38	42.26	28.35	25.92	23.71	20.87	40.5	90.81	41.32	6.15	99.5	40.46	44.56
	+ OBCACHE-VALUE	26.26	29.7	48.15	52.43	41.66	28.27	26.29	24.06	21.03	40.5	91.58	41.72	6.31	99.5	41.16	44.63
	+ OBCACHE-KEY	25.43	32.48	47.27	52.91	41.66	28.94	25.61	23.93	21.17	41.5	91.13	41.69	6.31	99.5	41.6	45.24
	+ OBCACHE-JOINT	25.61	32.2	49.47	53.31	41.58	28.22	26.34	23.69	21.28	41.0	90.78	41.53	6.31	99.5	41.26	45.16
	TOVA	26.27	24.83	44.48	52.69	39.04	28.68	25.0	22.96	20.71	41.0	92.16	42.28	6.31	99.5	37.35	35.21
	+ OBCACHE-VALUE	26.41	25.76	45.03	53.0	39.61	28.5	25.12	22.93	20.77	42.0	92.66	42.49	6.31	99.5	37.33	35.56
	+ OBCACHE-KEY	26.71	25.72	45.89	53.3	40.61	28.85	25.39	22.55	20.35	43.0	91.68	41.96	6.31	99.5	37.02	34.29
	+ OBCACHE-JOINT	25.93	25.88	43.6	53.03	39.89	28.13	25.23	23.09	20.77	42.0	91.61	42.24	6.31	99.5	38.15	36.3
	SnapKV	26.34	35.2	54.33	54.41	42.96	30.06	25.84	24.06	20.28	67.5	91.72	41.64	6.31	99.5	42.82	46.58
	+ OBCACHE-VALUE	26.59	35.34	51.69	55.03	42.3	30.03	26.05	24.73	20.25	66.0	91.68	41.66	6.31	99.5	42.82	46.47
	+ OBCACHE-KEY	27.01	36.25	52.22	55.2	42.86	30.39	26.3	24.42	20.47	68.0	90.72	41.35	6.31	99.5	42.57	47.5
	+ OBCACHE-JOINT	26.8	35.22	53.27	54.74	43.33	30.47	26.13	24.48	20.56	67.5	91.34	41.34	6.31	99.5	42.9	47.07
10% KV	H2O	26.94	31.95	49.83	53.37	44.41	29.22	27.4	23.86	22.05	43.5	91.51	42.3	6.31	99.5	47.35	46.99
	+ OBCACHE-VALUE	27.55	32.65	50.55	53.99	45.25	30.2	27.33	23.61	21.67	43.5	91.83	42.24	6.31	99.5	48.02	46.59
	+ OBCACHE-KEY	27.65	35.55	50.82	53.39	44.53	29.66	27.26	23.72	22.2	45.0	91.52	42.18	6.31	99.5	48.25	47.03
	+ OBCACHE-JOINT	27.53	34.29	52.17	53.65	44.71	29.63	27.76	23.84	22.19	44.0	91.51	43.07	6.31	99.5	48.21	47.01
	TOVA	27.11	28.51	48.16	54.13	39.84	28.24	26.66	23.0	21.41	46.0	92.13	42.34	6.31	99.5	41.32	38.36
	+ OBCACHE-VALUE	26.35	29.23	47.19	54.58	40.09	28.92	26.56	23.22	21.46	46.5	91.68	42.82	6.31	99.5	41.21	38.99
	+ OBCACHE-KEY	26.94	29.93	49.25	54.31	40.3	28.87	26.73	23.18	21.51	47.5	91.78	42.44	6.31	99.5	41.04	39.36
	+ OBCACHE-JOINT	26.18	29.78	49.22	54.3	40.73	29.19	26.47	23.71	21.5	47.0	91.47	42.79	6.31	99.5	41.57	39.17
	SnapKV	28.09	37.95	53.65	55.08	43.53	30.17	27.79	24.41	22.2	67.5	91.97	42.27	6.31	99.5	50.07	48.09
	+ OBCACHE-VALUE	28.38	37.77	53.89	55.67	43.0	30.05	27.7	23.96	22.57	68.0	91.97	43.5	6.31	99.5	49.99	48.48
	+ OBCACHE-KEY	28.22	39.71	53.44	54.98	44.12	30.24	27.96	24.37	22.73	68.5	91.18	42.58	6.31	99.5	50.18	48.61
	+ OBCACHE-JOINT	28.69	38.2	53.92	55.33	44.1	30.35	27.63	24.38	22.6	67.5	91.75	43.16	6.31	99.5	49.46	48.5
20% KV	H2O	28.9	35.96	51.73	55.63	44.3	29.69	29.39	24.04	23.03	47.5	91.27	42.31	6.31	99.5	50.1	48.46
	+ OBCACHE-VALUE	28.78	37.19	52.51	55.0	45.19	30.49	29.34	24.32	23.3	48.0	91.77	42.71	6.56	99.5	51.43	47.9
	+ OBCACHE-KEY	28.36	37.41	52.65	54.98	44.82	29.87	29.17	24.38	23.31	50.0	91.74	42.8	6.31	99.5	51.34	48.38
	+ OBCACHE-JOINT	28.26	38.42	53.47	55.38	44.92	29.99	29.11	24.23	23.09	48.5	91.44	42.66	6.31	99.5	51.45	48.22
	TOVA	27.47	33.83	52.88	53.79	41.74	29.57	28.94	23.61	22.71	62.0	91.59	42.2	6.31	99.5	44.34	41.7
	+ OBCACHE-VALUE	27.15	34.42	52.38	54.54	42.22	30.47	28.92	23.59	23.02	62.5	91.39	42.67	6.31	99.5	44.41	42.7
	+ OBCACHE-KEY	27.52	35.09	52.09	53.8	42.42	30.14	28.85	23.63	23.06	62.0	91.39	42.4	6.31	99.5	45.36	43.05
	+ OBCACHE-JOINT	27.11	34.97	52.29	54.35	42.39	30.14	29.03	23.56	23.05	62.0	91.83	42.16	6.31	99.5	44.87	42.45
	SnapKV	28.39	42.19	53.74	55.42	43.93	30.44	29.86	24.51	23.86	70.5	91.74	42.46	6.31	99.5	52.22	48.64
	+ OBCACHE-VALUE	29.19	41.86	53.95	55.43	44.54	29.94	29.76	24.77	23.64	69.0	91.73	43.18	6.31	99.5	52.06	49.04
	+ OBCACHE-KEY	29.53	42.71	54.81	55.24	44.65	30.13	29.85	24.37	24.11	69.5	91.91	42.9	6.31	99.5	52.14	48.63
	+ OBCACHE-JOINT	28.78	40.9	54.08	55.25	44.34	30.51	29.79	24.33	23.87	69.5	91.56	43.2	6.56	99.5	52.55	49.19

Table 3: LongBench results for Qwen-2.5-7B-Instruct.

Methods	Single-Document QA			Multi-Document QA			Summarization			Few-shot Learning			Synthetic		Code		
	NrvQA	Qasper	MF-en	HotpotQA	2WikiMQA	Musique	GovReport	QMSum	MultiNews	TREC	TriviaQA	SAMSum	PCount	Pre	Lec	RB-P	
ALL KV	29.16	43.24	52.94	58.87	48.15	31.06	32.65	23.65	24.22	72.5	89.28	45.51	8.5	100.0	58.23	65.28	
5% KV	H2O	27.99	32.24	42.15	52.91	43.3	27.25	24.61	22.59	17.84	36.0	87.06	44.32	9.0	100.0	45.61	56.48
	+ OBCACHE-VALUE	28.32	33.12	43.53	52.7	42.62	25.68	24.98	22.82	18.33	36.0	86.9	44.0	9.0	100.0	45.63	57.01
	+ OBCACHE-KEY	28.2	32.49	42.91	53.82	42.62	26.88	25.27	22.76	18.38	36.5	87.38	43.78	9.0	100.0	44.57	57.06
	+ OBCACHE-JOINT	28.15	32.53	45.02	53.52	43.94	28.2	25.1	23.01	18.28	36.0	87.74	44.4	9.0	100.0	45.59	56.95
	TOVA	21.07	26.32	36.87	51.0	38.78	29.6	23.7	21.14	17.09	36.0	87.0	44.8	9.0	100.0	41.09	45.24
	+ OBCACHE-VALUE	23.0	27.32	35.91	51.66	40.14	29.01	23.88	21.43	17.13	39.5	87.07	44.58	9.0	100.0	44.03	46.58
	+ OBCACHE-KEY	22.93	27.52	35.06	51.67	40.27	29.52	23.91	21.27	17.26	41.5	87.05	44.76	9.0	100.0	43.06	46.88
	+ OBCACHE-JOINT	23.24	27.09	36.47	51.18	39.53	29.7	24.07	21.19	17.22	39.0	87.49	44.89	9.0	100.0	44.1	46.39
	SnapKV	29.19	36.57	51.76	55.6	46.56	30.23	25.09	22.95	17.23	68.0	87.37	43.69	9.0	100.0	45.98	58.74
	+ OBCACHE-VALUE	28.96	37.73	51.36	55.55	45.94	30.98	25.14	22.75	17.49	68.5	87.6	43.35	9.0	100.0	46.8	59.42
	+ OBCACHE-KEY	29.9	36.88	51.05	55.08	45.36	30.47	25.37	22.42	17.4	65.0	87.41	43.43	9.0	100.0	47.88	59.72
	+ OBCACHE-JOINT	28.82	36.84	49.92	55.65	45.5	30.59	25.29	22.2	17.71	66.5	86.23	44.32	9.0	100.0	47.62	59.63
10% KV	H2O	28.48	36.71	45.76	52.66	43.73	28.8	26.54	22.84	19.2	39.5	88.34	45.09	9.0	100.0	53.24	61.41
	+ OBCACHE-VALUE	28.99	36.28	46.95	53.93	44.89	29.2	27.27	22.75	19.65	39.5	88.5	45.34	9.0	100.0	53.81	61.05
	+ OBCACHE-KEY	29.13	35.37	46.24	55.02	46.21	29.4	27.49	22.97	19.62	39.0	88.86	44.5	9.0	100.0	54.17	61.23
	+ OBCACHE-JOINT	29.23	36.46	46.43	55.01	44.16	29.06	27.04	22.74	19.74	40.0	89.08	45.43	9.0	100.0	53.72	61.1
	TOVA	25.96	31.33	41.37	52.9	42.87	30.31	26.15	21.84	18.34	54.0	87.13	45.24	9.0	100.0	45.49	48.63
	+ OBCACHE-VALUE	27.28	32.21	41.26	53.36	44.01	29.48	26.21	21.93	18.4	57.0	87.03	45.71	9.0	100.0	45.35	48.77
	+ OBCACHE-KEY	26.2	30.62	43.15	53.87	41.72	29.39	26.34	21.82	18.76	56.0	87.13	45.46	9.0	100.0	45.99	51.34
	+ OBCACHE-JOINT	27.07	31.65	41.02	53.54	42.75	29.26	<									